MCNPX SIMULATIONS FOR POSITRON PRODUCTION MECHANISMS TO GENERATE DEFECT DENSITY IMAGES USING POSITRON ANNIHILATION ENERGY SPECTROSCOPY

V. Makarashvili, D. P. Wells

Department of Physics, Idaho State University, Campus Box 8106, Pocatello, ID 83209 makavakh@isu.edu

MCNPX simulations were performed as an attempt to quantitatively characterize possible positron production mechanisms coupled with Positron Annihilation Energy Spectroscopy (PAES). Based on the simulation results and the previous experiments performed by A. Hunt, et al. it was decided to choose the PAES technique coupled with pair production method of positron creation using bremsstrahlung photon beams from a linear accelerator to generate defect density images of large scale structural materials.

I. INTRODUCTION

Positron Annihilation Spectroscopy (PAS) techniques can be utilized to detect and study sub-nanoscale defects. These kinds of defects are often very important to the formation of macroscopic damage or material failure. As a result, PAS methods could be an excellent non-destructive probe for identifying damage in structural materials, before the physical damage signs are present.

Our objective is to demonstrate the capabilities of the PAS techniques to generate 2D and possibly 3D defect images (defect density plots) for large structural materials widely used in industry.

In order to achieve this goal, we need to pick a suitable positron production source and a proper PAS technique. MCNPX simulations were performed as an attempt to quantitatively characterize possible positron production mechanisms coupled with Positron Annihilation Energy Spectroscopy (PAES).

II. MCNPX RESULTS

II.A ^{27}Al(p, γ)^{28}Si Reaction

To perform simulations on the ^{27}Al(p, γ)^{28}Si reaction, first we had to generate the emission gamma spectrum from the reaction, which was done by combining the published counting rates and cross-sections for all the capture resonances (below 1 MeV) and all the decay schemes with corresponding branching ratios.[1, 2, 3] Fig. 1 shows the gamma emission spectrum of the reaction, the result of this data analysis.

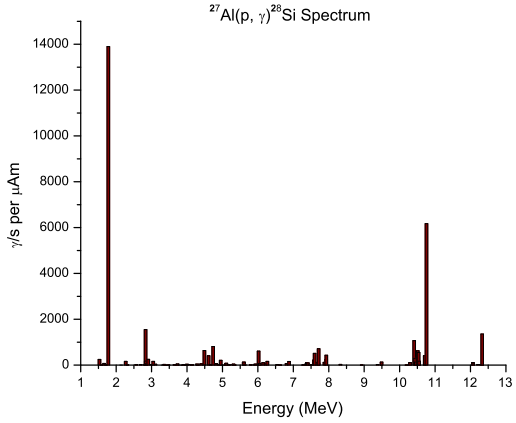

Fig. 1. Emission spectrum of the ^{27}Al(p, γ)^{28}Si reaction from 1 MeV proton bombardment on an aluminum target.

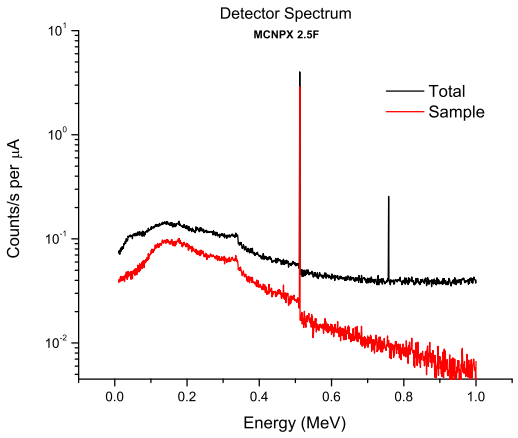

Fig. 2. Detector spectrum from MCNPX

This spectrum was put in the MCNPX source definition as the energy distribution function of the gammas. These source gammas were emitted isotropically from a 0.3 cm radius and $1.4 \cdot 10^{-3}$ cm (which is approximately the range of 1 MeV protons in Al) thick

aluminum disk. A Ge detector crystal was modeled according to the coaxial geometry as a cylinder with 5.9 cm diameter and 8.3 cm long (corresponds to about 80% relative efficiency). The sample in our simulations was chosen to be 3x3x3 cm^3 stainless steel. We simulated several different configurations with different thicknesses of lead shielding around the detector and different orientation of the detector. However, it turned out that the best configuration was placing detector right next to the aluminum target with no shielding at all. See Fig. 2 for the results of MCNPX simulations with this configuration.

The 511 keV gamma counting rates were low: 2.89 ± 0.02 counts/s and 1.13 ± 0.01 counts/s (per μA of the proton beam) for the sample and the background (not from sample) respectively. Note that, induced radioactivity of the sample is essentially zero.

II.B Bremsstrahlung

Fig. 3 demonstrates the setup that was used for bremsstrahlung simulations. Electrons were emitted mono-directionally from the electron LINAC made out of stainless steel. They were converted into bremsstrahlung photons by a 2 mm thick tungsten converter. The bremsstrahlung photons were collimated using two collimators in a 1.2 m thick concrete wall. We used the same sample and detector crystal models as in the previous simulations. This time the detector had lead shield with a 2 cm diameter collimator.

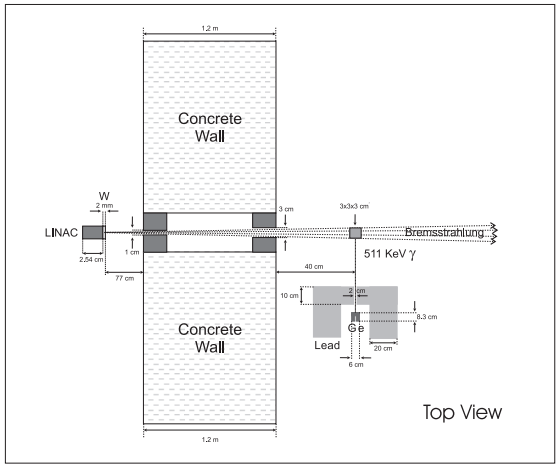

Fig. 3. MCNPX geometry for bremsstrahlung

It was inefficient to simulate everything in a single run, because one can only run $2 \cdot 10^9$ source particles in MCNPX in a single run, which wasn't enough to generate significant 511 keV gammas in the detector. Thus, we split the problem in two parts. The first part gave us the bremsstrahlung energy distribution in the sample, while the second part produced e^+ - e^- pairs from pair production that, in turn, produced 511 keV gammas from annihilation of the positrons. We used two electron energies for these simulations: 5 MeV and 15 MeV. The resulting detector spectra are presented on Fig. 4 and Fig. 5 respectively.

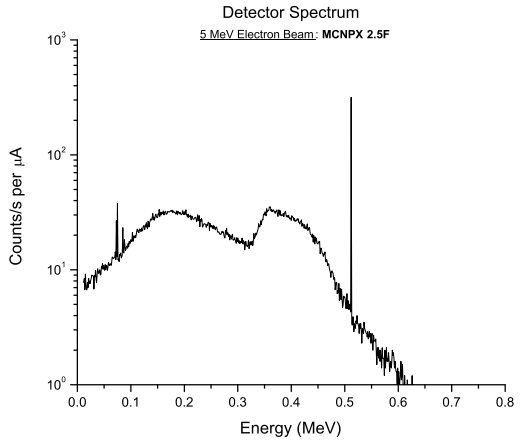

Fig. 4. MCNPX spectrum for 5 MeV electron beam, bremsstrahlung photons below 1 MeV were not tracked.

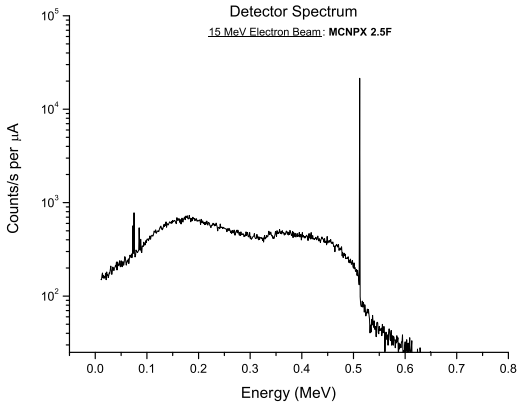

Fig. 5. MCNPX spectrum for 15 MeV electron beam, bremsstrahlung photons below 1 MeV were not tracked

The detected 511 keV rates per μA of the electron beam were 317 ± 5 counts/s and 21400 ± 200 counts/s for 5 MeV and 15 MeV respectively. There are no background 511 keV gammas present. The radioactivity of the sample for a 15 MeV run can be neglected.

II.C Activation

Estimating the counting rates for the activation technique with iron alloys was more challenging than in the previous two cases. First, we had to calculate the following integral numerically, which represents the $^{54}Fe(\gamma, n)^{53}Fe$ reaction rate:

$$k = N\int_{12}^{22}\frac{d\phi(E)}{dE}\sigma(E)dE \qquad (1)$$

The flux was found from the MCNPX simulations and the cross-section was taken from the literature.[4] We used the same simulation models for the electron LINAC, the tungsten converter and the sample. The distance between the converter and the sample was about 5 cm and the energy of the electrons was 22 MeV. The reaction rate k was determined for 1 μA of electron beam.

After evaluating the integral numerically we were able to find the number of ^{53}Fe nuclei produced as a function of time.

$$N(t) = \frac{k}{\lambda}\left(1 - e^{-\lambda t}\right) \qquad (2)$$

The function was determined by using simple serial transformation of the process:

$$^{54}Fe \xrightarrow{k} {}^{53}Fe \xrightarrow{\lambda} {}^{53}Mn$$

The population function is shown on Fig. 6

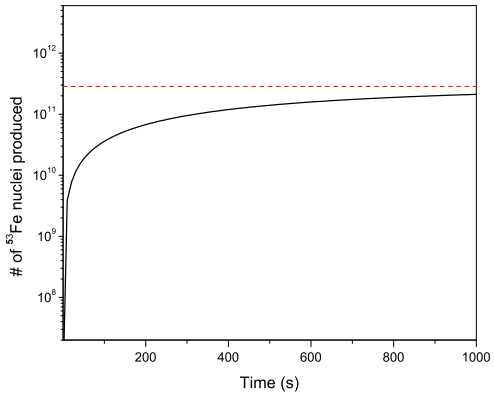

Fig. 6. Number of ^{53}Fe nuclei as a function of time

The average rate of positrons and the activity of the sample after 10 min activation and 10 min decay were found to be $(7.3 \pm 0.4)\cdot 10^7$ positrons per second and 5.8 ± 0.3 mCi respectively based on Fig. 6. Then the positron rate was converted to 511 keV counts/s by running one more MCNPX simulation. In this case 1 keV (lower energy cutoff for electrons/positrons in MCNPX) mono-energetic positrons were randomly distributed in the sample as source particles and number of 511 keV photons per positron was counted in the detector. The data is presented in Fig. 7

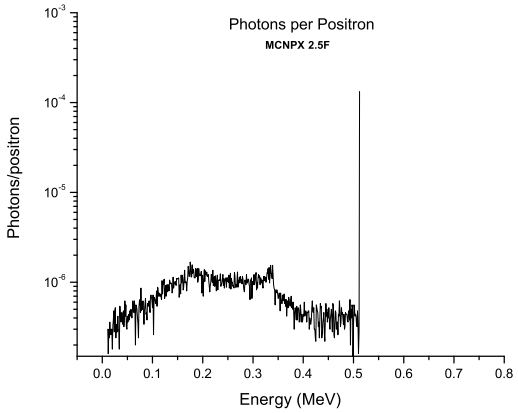

Fig. 7. Number of photons detected per positron from MCNPX

Finally, we estimated the 511 keV count rate, which was 9500 ± 500 counts/s.

The results of the MCNPX simulations are summarized in Table 1.

TABLE I. Summary of the MCNPX simulations

TECHNIQUE		Rate (c/s)	BKG (c/s)	A (mCi)
$^{27}Al(p, \gamma)^{28}Si$		2.89	1.13	0
Bremss.	5 MeV	317	0	0
	15 MeV	21400	0	0
Activation		9500	0	5.8

As we can clearly see, the $^{27}Al(p, \gamma)^{28}Si$ reaction is not competitive due to the low counting rates. It's difficult to make a decision between bremsstrahlung and activation by only looking at the count rates. So, we have to rely on the qualitative judgment and the knowledge from previous experiments.[5-8]

The following limitations of the photo activation mechanism have been noticed by A. W. Hunt et. al in 2004 at ISU.[9] After irradiation the samples become radioactive and cause a potential radiation safety concern.

Most importantly, the constituent nuclei of the sample must be suitable for photo activation. This implies that, the positron emitting radioisotope, produced in (γ, n) reactions must have appropriate activity and half-life. Also, any additional radioisotopes produced in the material must not interfere with the annihilation line by producing high count rates in the detector.

The pair production technique using bremsstrahlung photon beams overcomes the above mentioned limitations of photo activation method mainly because it does not depend on photo-nuclear reactions, but, rather, photo-atomic reaction. It seems that, combining this technique with regular PAES is the most promising approach to achieve our goals.

III. FUTURE WORK

A linear accelerator (LINAC) will be employed to conduct experiments that "test" these simulations. The accelerator is capable of producing 15 MeV electron beams with 30-60 ns pulse width, up to 200 mA peak current at 1 kHz repetition rate. The electron beam from the accelerator gets converted into a bremsstrahlung beam using a 2-3 mm thick tungsten converter. The highly collimated photons travel through a 1.2 m (about 4 feet) thick concrete wall that has two collimators. The size and the shape of the collimators will be selected according to the size of the sample and the setup geometry. We would like to acquire a flat (so called fan) beam that entirely covers a 2D slice of the sample. Our proposed samples are cylindrical bundles of steel rods, some of them having induced mechanical damage.

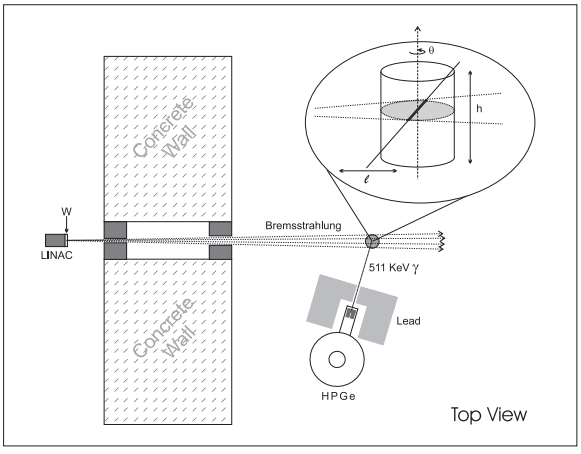

Fig. 8. Proposed experimental setup

A HPGe (about 20% relative efficiency) will be used to detect annihilation radiation. The detector will be shielded and collimated such that it only 'sees' a small linear section of the irradiated 2D slice (See Fig. 8.). The samples will be translated horizontally (by Δl), in order to cover the entire irradiated slice. The spectra will be obtained for each position of this horizontal scan. After completing this step the samples will be rotated with small increments (Δθ) until we cover 180^0 degree angle (actually, it's going to be less than 180^0, because of the fan-beam geometry). Similarly, the spectra will be obtained for each increment of the angular scan. The irradiation plane has to be translated in the vertical direction (by Δh), covering the whole length of the cylinder and the (l, θ) scan has to be performed for each plane, in order to generate 3D images. The scanning parameters Δl, Δθ , and Δh, that limit the spatial resolution and the image quality of the imaging technique, will be determined after the preliminary experiments.

The parameters of the 511 keV peak that characterize the defects: S and W, will be determined for each scanning position. In other words, these parameters will be as functions of l, θ and h.

$$S = g(l,\theta;h) \text{ or } W = g(l,\theta;h) \qquad (3)$$

By plotting the g(l, θ) for each h, we should be able to generate sinograms of the scanned samples. Imaging software (IDL, or similar) will be used to reconstruct our images from the sinograms, using one of the reconstruction algorithms (Fourier method, filtered backprojection or convolution backprojection) taking into the account the fan-beam geometry.

Samples, with different degrees of damage and different configuration, will be studied to identify defects on the reconstructed images and to investigate possible strength and limitations of the proposed method.

IV. CONCLUSIONS

The PAES technique coupled with pair production method of positron creation using bremsstrahlung photon beams from a linear accelerator seems to be the most promising tool to achieve 3-D defect density imaging. A high duty factor linear accelerator would improve this considerably. Other candidate techniques, namely (p, γ) and (γ, n) reactions, were also simulated in this work.

ACKNOWLEDGMENTS

This work was funded by a grant from DOE
DE-FC07-Q6ID14780

REFERENCES

1. S. HARISSOPULOS, C. CHRONIDOU, K. SPYROU, T. PARADELLIS, C. ROLFS, W. H. SCHULTE, H. W. BECKER "The ^{27}Al(p, γ)^{28}Si reaction: direct capture cross-section and resonance strength at E_p = 0.2 – 1.12 MeV" *Eur. Phys. Journal A,* Vol. **9** pp. 479-489, December 2000
2. C. CHRONIDOU, K. SPYROU, S. HARISSOPULOS, S. KOSSIONIDES, T. PARADELLIS "Resonance strength measurement of the ^{27}Al(p, γ)^{28}Si reaction in the energy range E_p = 0.8 – 2.0 MeV" *Eur. Phys. Journal A,* Vol. **6** pp. 303-308, August 1999
3. P. M ENDT, C. VAN DER LEUN "Energy levels of Z = 11 – 21 nuclei (IV)" *Nuclear Physics A,* Vol. **105**, Issue **1**, pp. 139-142, December 1967
4. J. W. NORBURY, M. N. THOMPSON, K. SHODA, H. TSUBOTA "Photoneutron cross section of Fe-54." *Australian Journal of Physics*; Vol.**31**, p.471, 1978
5. F. A. SELIM, D. P. WELLS, J. F. HARMON, J. WILLIAMS "Development of accelerator-based γ-ray-induced positron annihilation spectroscopy technique" *Journal of Applied Physics* Vol. **97**, pp. 113539-113539-5, 2005
6. F. A. SELIM, D. P. WELLS, J. F. HARMON, J. KWOFIE, G. ERIKSON, T. RONEY "New positron annihilation spectroscopy techniques for thick materials" *Radiation Physics and Chemistry* Vol. **68** pp. 427-430, 2003
7. F. A. SELIM, D. P. WELLS, J. F. HARMON, W. SCATES, J. KWOFIE, R. SPAULDING, S. P. DUTTAGUPTA, J. L. JONES, T. WHITE, T. RONEY "Doppler broadening measurements of positron annihilation using bremsstrahlung radiation" *Nuclear Instruments and Methods in Physics Research, Section B* Vol. **192**, pp. 197-201, 2002
8. F. A. SELIM, D. P. WELLS, J. F. HARMON "Positron lifetime measurements by proton capture" *Review of Scientific Instruments* Vol. **76**, pp. 033905-033905-3, 2005
9. A. HUNT, R. SPAULDING, J. URBAN-KLAEHN, J. F. HARMON, D. P. WELLS "Defect imaging of structural objects using positron annihilation spectroscopy" *Nuclear Inst. and Methods in Physics Research, Section B*, Vol. **241** pp 262-262, Dec. 2005
10. MCNPX^{TM} Users Manual, 2.5.0 *LA-CP-05-0369*